# NACA

# RESEARCH MEMORANDUM

*Ref # 5164*

23 MAR 1956

## A FREE-FLIGHT INVESTIGATION OF THE EFFECTS OF A SONIC JET

## ON THE TOTAL-DRAG AND BASE-PRESSURE COEFFICIENTS

## OF A BOATTAIL BODY OF REVOLUTION FROM

## MACH NUMBER 0.83 TO 1.70

By Ralph A. Falanga

Langley Aeronautical Laboratory
Langley Field, Va.

# NATIONAL ADVISORY COMMITTEE
# FOR AERONAUTICS
## WASHINGTON
March 8, 1956

CONFIDENTIAL

## NATIONAL ADVISORY COMMITTEE FOR AERONAUTICS

### RESEARCH MEMORANDUM

## A FREE-FLIGHT INVESTIGATION OF THE EFFECTS OF A SONIC JET

## ON THE TOTAL-DRAG AND BASE-PRESSURE COEFFICIENTS

## OF A BOATTAIL BODY OF REVOLUTION FROM

## MACH NUMBER 0.83 TO 1.70

### By Ralph A. Falanga

### SUMMARY

Two 7.5° conical boattail bodies of revolution with constant base annuli and varying jet static-pressure ratios and with simulated turbo-jet exhaust rocket motors were flight-tested to determine the jet inter-ference effects on total-drag and base-pressure coefficients over a Mach number range from approximately 0.83 to 1.70. The results indicated that for jet static-pressure ratios of 1.83 to 2.40, power-on total-drag coefficients were lower than the corresponding power-off values through-out the test Mach number range. The lower jet static-pressure ratio indicated less difference between power-off and power-on total-drag coef-ficients as well as reduced power-on base-pressure coefficients.

### INTRODUCTION

With the penetration of modern high-speed airplanes into supersonic flight regime, considerable interest is being directed toward the effects that propulsive jets have on external drag of nacelles and fuselage after-bodies and on the base pressures around the jet exit. Data on base pres-sures and boattail drag (refs. 1 to 6) have shown that power-on drag coef-ficients may be considerably lower than the power-off drag coefficients. The magnitude of the difference in drag coefficients depends on the afterbody-geometry, nozzle-design, and jet-operating conditions.

Inasmuch as there is no adequate analytical method available other than the semiempirical theories for calculating or predicting base pres-sures, the Langley Pilotless Aircraft Research Division is currently con-ducting flight tests to determine the effects of a sonic turbojet exhaust on body base pressure and total drag at transonic and supersonic speeds.

CONFIDENTIAL

The initial results, reported in reference 6, simulated a sonic turbojet exhaust at 35,000 feet altitude. The present investigation utilizes lower jet static-pressure ratios which correspond to flight at lower altitude.

Two research models with identical configuration, but with different jet static-pressure ratios, propelled with turbojet simulators (designed according to ref. 7) were flight-tested at Langley Pilotless Aircraft Research Station, Wallops Island, Va. Power-on data for model 1 covered a Mach number range from 0.90 to 1.15 and Reynolds number range, based on body length, from $28.70 \times 10^6$ to $35.00 \times 10^6$, while that of model 2 covered a Mach number range from 1.4 to 1.70 and Reynolds number range from $52.25 \times 10^6$ to $59.00 \times 10^6$.

## SYMBOLS

A       area, sq ft

a       acceleration, $ft/sec^2$

D       drag, lb

g       acceleration due to gravity, $ft/sec^2$

M       Mach number

p       static pressure, $lb/ft^2$ abs

$q_o$       dynamic pressure, $\dfrac{\gamma p_o M_o^2}{2}$, $lb/ft^2$

R       Reynolds number based on body length

S       maximum cross-sectional area, $ft^2$

$T_j$       thrust, $p_j A_j \left( \gamma M_j^2 + 1 \right) - p_o A_j$

W       weight, lb

$\theta$       flight-path angle, deg

$\gamma$       ratio of specific heats

$C_{p_b}$       base-pressure coefficient, $\dfrac{p_b - p_o}{q_o}$

$C_{D_{off}}$      power-off drag coefficient, $\dfrac{D}{q_o S}$

$C_{D_{on}}$      power-on drag coefficient, $\dfrac{T_j - W_i\left(\dfrac{a_L}{g} + \sin\theta\right)}{q_o S}$

$C_{D_{b_{off}}}$      power-off base drag coefficient, $-C_{p_b}\dfrac{A_b}{S}$

$C_{D_{b_{on}}}$      power-on base drag coefficient, $-C_{p_b}\dfrac{A_a}{S}$

Subscripts:

o      free stream

j      jet exit

b      base

t      rocket throat

a      base annulus

i      instantaneous

L      longitudinal


## DESCRIPTION OF MODELS

Models 1 and 2 (identical with model 2 of ref. 6) had a ratio of jet-to-base area of 0.706 and differed only in jet static-pressure ratios and power-on test Mach number range covered. Details and dimensions of the configurations are given in figure 1.

The parabolic nose section, coordinates of which are given in table I, was 26.00 inches long, and the straight cylindrical section was 28.03 inches in length. The conical afterbody had a $7.5°$ boattail angle and was 10.97 inches long. Four thin $60°$ sweptback fins with beveled leading and trailing edges attached to the conical afterbody were used to stabilize the body in flight. The body total length was 65 inches for the two models and had a fineness ratio of 10.

Figure 2 shows a cross section of a typical turbojet simulator and listed in this figure are the throat and exit diameters of the simulators. The technique and operation of the simulator are described in reference 7.

Test Techniques and Instrumentation

The models were launched from a rail-type launcher at approximately
a 55° angle as shown in figure 3. Single 65-inch HVAR rocket motors
boosted each model to supersonic speeds. The turbojet simulator of
model 2 was programmed to fire at a different flight time from that of
model 1 in order to extend the Mach number range of the power-on phase.
The variation of Mach number with time for the present flight models is
presented in figure 4.

A four-channel telemeter which was carried in the nose of each model
continuously transmitted measurements of base static pressure, motor
static pressure, and low- and high-range longitudinal accelerometer data
to the ground receiving stations. Flight data were also obtained from
CW Doppler velocimeter, NACA modified SCR 584 tracking radar, tracking
cameras, and radiosonde. These data were used to obtain total-drag coef-
ficients, Mach number, and free-stream static pressure (by methods
described in ref. 8) as well as base-pressure and base drag coefficients.
Base pressures were measured at the orifice shown in figure 2.

Static firings were performed on each of the turbojet simulators
used in the flight models to determine whether each unit met the speci-
fied engine parameters. Reference 7 gives methods used in determining
and simulating required engine exit parameters. A calibration curve of
jet exit static pressure $p_j$ was established from these tests as a

function of a motor-static pressure whose orifice location is as shown
in figure 2. These calibration curves were then used along with measure-
ments of motor static pressure and free-stream static pressure to obtain
the thrust during flight.


TEST ACCURACY


The basic accuracy of the power-off total-drag coefficients and base-
pressure coefficients presented herein has been established by comparison
of the individual drag and base-pressure coefficient curves of five simi-
lar models. Any deviation in drag and base-pressure coefficients which
existed in these curves could have been caused by model dissimilarities
in construction and finish, and/or instrumentation errors of the CW
Doppler velocimeter, tracking radar, telemeter, and radiosonde. The
maximum measured differences of drag and base-pressure coefficients
between the five similar models are tabulated as follows for power-off
condition.

| M | ΔM | $C_{p_b}$ | $C_D$ |
|---|---|---|---|
| 0.95 | ±0.010 | ±0.0140 | ±0.0145 |
| 1.25 | ±.005 | ±.0100 | ±.0080 |
| 1.40 | ±.005 | ±.0100 | ±.0095 |

The degree of accuracy obtained for computed power-on drag coefficients was based mainly on the accuracy with which the thrust of the rocket motors was computed, since the absolute values of the thrust were four to six times greater than those of the drag for all models tested. A maximum probable error of ±10 pounds of thrust was estimated for the technique used in obtaining absolute values of flight thrust. This corresponds to an error (due to thrust alone) in power-on drag coefficients of ±0.04 at M = 0.95 and ±0.03 at M = 1.150 for model 1. It is felt, based upon past experience, that the level of measured experimental data is better than that which the maximum probable error indicates.

## RESULTS AND DISCUSSION

The Mach number range covered by these flight models was from 0.83 to 1.70. The Reynolds number, based on body length, varied from $25.25 \times 10^6$ to $59.70 \times 10^6$ for power-off period and from $28.7 \times 10^6$ to $59.00 \times 10^6$ for power-on period as shown in figure 5. The range of Reynolds number covered by both models indicates that the boundary layer near the base was turbulent.

The variation of total-drag coefficient, base-drag coefficient, and base-pressure coefficient (for power-off and power-on) and jet static-pressure ratio with free-stream Mach number are presented in figures 6 and 7 for models 1 and 2, respectively. The motor static-pressure cell of model 2 did not function properly in flight, hence, the power-on drag coefficient and jet static-pressure ratio curves for this model were not obtained.

An estimated $p_j/p_0$ curve shown in figure 7(c) was obtained from preflight test results and knowledge of the power-on duration of the turbojet simulator of model 2 in flight. Based on the method used, it is felt that the estimated curve is within 5 percent of the actual curve.

## Total Drag

Jet interference effects on body drag of model 1 resulted in lower power-on drag coefficient values throughout the flight-test Mach number range. Between $M = 0.92$ and $M = 1.00$, the reduction in drag is greater than the reduction at the low supersonic speeds. At the low supersonic speeds, the reduction in drag is approximately equal to the magnitude of the difference of base drag from power-off to power-on whereas, at the lower speeds, the difference that exists is greater than the change in base drag alone. It is felt that positive pressure increments acted on part of the boattail to cause this noted reduction in drag at the lower speeds ($M = 0.92$ to $1.00$). This same effect has been noted in references 5, 6, and 9.

The effect on total drag of varying the jet static-pressure ratio is illustrated in figure 8(a) which compares power-off and power-on total-drag coefficients of model 1 with model 2 of reference 6. The power-off total-drag coefficient curve presented in this plot was obtained by averaging $C_{D_{off}}$ of the present models and model 2 of reference 6. Model 2 of reference 6 had the same external configuration as the present test models, but differed in jet pressure ratio and henceforth will be referred to as reference 6 in the text and plots. The jet static-pressure ratio of model 1 varied from 1.83 at $M = 0.90$ to 2.40 at $M = 1.15$, while reference 6 was relatively constant at 3.70 throughout its test Mach number range. Thus, it is indicated that increasing the jet static-pressure ratio appears to decrease the total drag coefficient.

## Base-Pressure and Base-Drag Coefficients

Coefficients of base pressure for the power-on phases remain positive (in the direction of thrust) throughout the test Mach number range whereas, the power-off base-pressure coefficients are positive below $M = 1.00$ and then become negative throughout the rest of the test Mach number range as can be observed in figures 6(b) and 7(b) for models 1 and 2, respectively. As shown in figures 6(a) and 7(a) for models 1 and 2, coefficients of base drag for power-off and power-on show the same trend. It should be noted in these plots that the base-drag coefficients were computed using the exposed area of the base. For example, during the power-off phase the entire base area was exposed, whereas during the power-on phase only the annulus area (base-minus-jet area) was exposed.

Reference 6 showed a somewhat greater difference between power-on and power-off base-drag coefficients than the present test models. This difference was probably due to the difference in jet static-pressure ratios. Figure 8(b) compares power-off and power-on base-pressure coefficients of models 1 and 2 with reference 6. This comparison illustrates

the effects of varying the jet static-pressure ratio on base-pressure coefficients. The lower jet static-pressure ratio of models 1 and 2 resulted in lower positive values of base-pressure coefficients.

In order to show the separate effects of Mach number and jet static-pressure ratio on the power-on base-pressure coefficients the data have been cross plotted in figure 9. Figure 9 shows the variation of power-on base-pressure coefficient with jet static-pressure ratio for three constant Mach numbers and the variation with free-stream Mach number for three constant jet-static-pressure ratios. It is indicated from these plots that power-on base-pressure coefficients not only become less positive with decreasing pressure ratio, as observed above, but also have a tendency to become less positive with supersonic Mach numbers.

<div align="center">CONCLUSIONS</div>

In summarizing the results of the present tests, certain findings are of particular interest. The results obtained from the two conical boattail bodies of revolution over the test Mach number range of 0.83 to 1.70 and Reynolds number range of $25.25 \times 10^6$ to $59.70 \times 10^6$ indicated the following:

1. For the jet static-pressure ratios tested, the effect of the jet was to reduce the total-drag coefficients throughout the test Mach number range, with the magnitude of drag reduction increasing with increasing jet static-pressure ratio.

2. Positive values of base-pressure coefficient were measured throughout the power-on test Mach number range.

3. Power-on base-pressure coefficients became less positive with a reduction of jet static-pressure ratios and also with increasing supersonic Mach numbers.

Langley Aeronautical Laboratory,
        National Advisory Committee for Aeronautics,
                Langley Field, Va., November 30, 1955.

## REFERENCES

1. DeMoraes, Carlos A., and Nowitsky, Albin M.: Experimental Effects of Propulsive Jets and Afterbody Configurations on the Zero-Lift Drag of Bodies of Revolution at a Mach Number of 1.59. NACA RM L54C16, 1954.

2. Love, Eugene S.: Aerodynamic Investigation of a Parabolic Body of Revolution at Mach Number of 1.92 and Some Effects of an Annular Jet Exhausting From the Base. NACA RM L9K09, 1950.

3. Cortright, Edgar M., Jr., and Kochendorfer, Fred D.: Jet Effects on Flow Over Afterbodies in Supersonic Stream. NACA RM E53H25, 1953.

4. Cortright, Edgar M., Jr., and Schroeder, Albert H.: Investigation at Mach Number 1.91 of Side and Base Pressure Distributions Over Conical Boattails Without and With Jet Flow Issuing From Base. NACA RM E51F26, 1951.

5. Henry, Beverly Z., Jr., and Cahn, Maurice S.: Preliminary Results of an Investigation at Transonic Speeds To Determine the Effects of a Heated Propulsive Jet on the Drag Characteristics of a Related Series of Afterbodies. NACA RM L55A24a, 1955.

6. Falanga, Ralph A.: A Free-Flight Investigation of the Effects of Simulated Sonic Turbojet Exhaust on the Drag of a Boattail Body With Various Jet Sizes From Mach Number 0.87 to 1.50. NACA RM L55F09a, 1955.

7. DeMoraes, Carlos A., Hagginbothom, William K., Jr., and Falanga, Ralph A.: Design and Evaluation of a Turbojet Exhaust Simulator, Utilizing a Solid-Propellant Rocket Motor, for Use in Free-Flight Aerodynamic Research Models. NACA RM L54I15, 1954.

8. Wallskog, Harvey A., and Hart, Roger G.: Investigation of the Drag of Blunt-Nosed Bodies of Revolution in Free Flight at Mach Numbers From 0.6 to 2.3. NACA RM L53D14a, 1953.

9. Englert, Gerald W., Vargo, Donald J., and Cubbison, Robert W.: Effect of Jet-Nozzle-Expansion Ratio on Drag of Parabolic Afterbodies. NACA RM E54B12, 1954.

TABLE I

COORDINATES OF PARABOLIC NOSE

[Station measured from fuselage nose]

| Station, in. | Ordinate, in. |
|:---:|:---:|
| 0 | 0 |
| 1 | .245 |
| 2 | .481 |
| 4 | .923 |
| 6 | 1.327 |
| 10 | 2.019 |
| 14 | 2.558 |
| 18 | 2.942 |
| 22 | 3.173 |
| 26 | 3.250 |
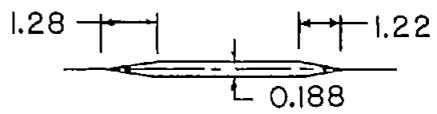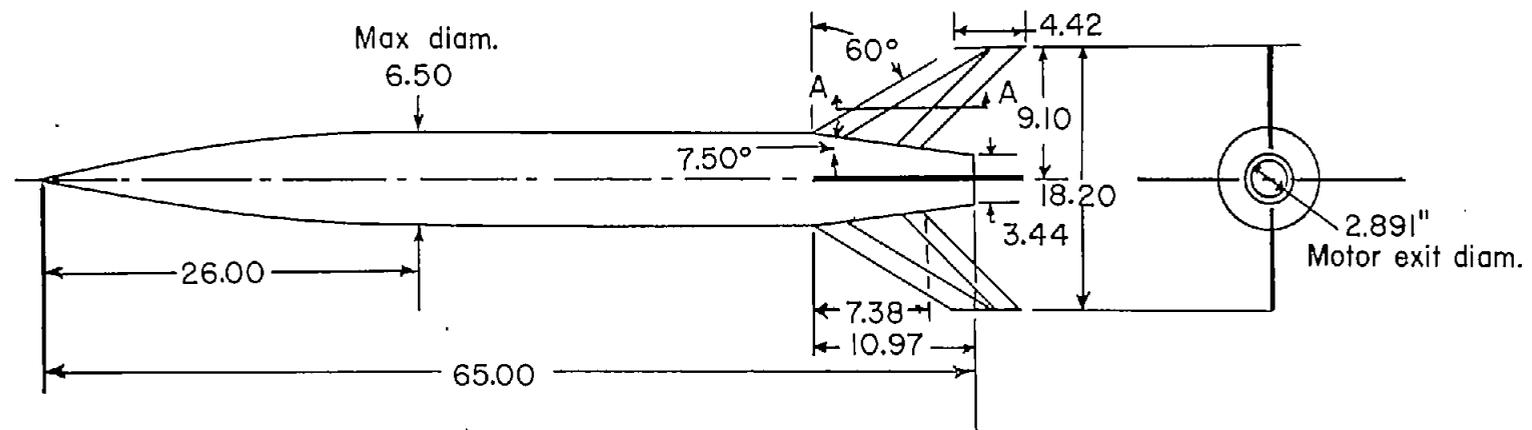
Figure 1.- External configuration of flight model. All dimensions are in inches.

Motor static-pressure orifice

Motor static-pressure tube

3.25" diam.

10"

A

Exit diam.

Rocket combustion chamber

Propellant

Grid

Nozzle

Base static-pressure orifice

Throat diameter

Plenum chamber

Base static-pressure tube

Igniter

| Model Number | Throat Diameter | Exit Diameter |
|---|---|---|
| 1 | 0.981" | 2.891" |
| 2 | 1.290" | 2.891" |
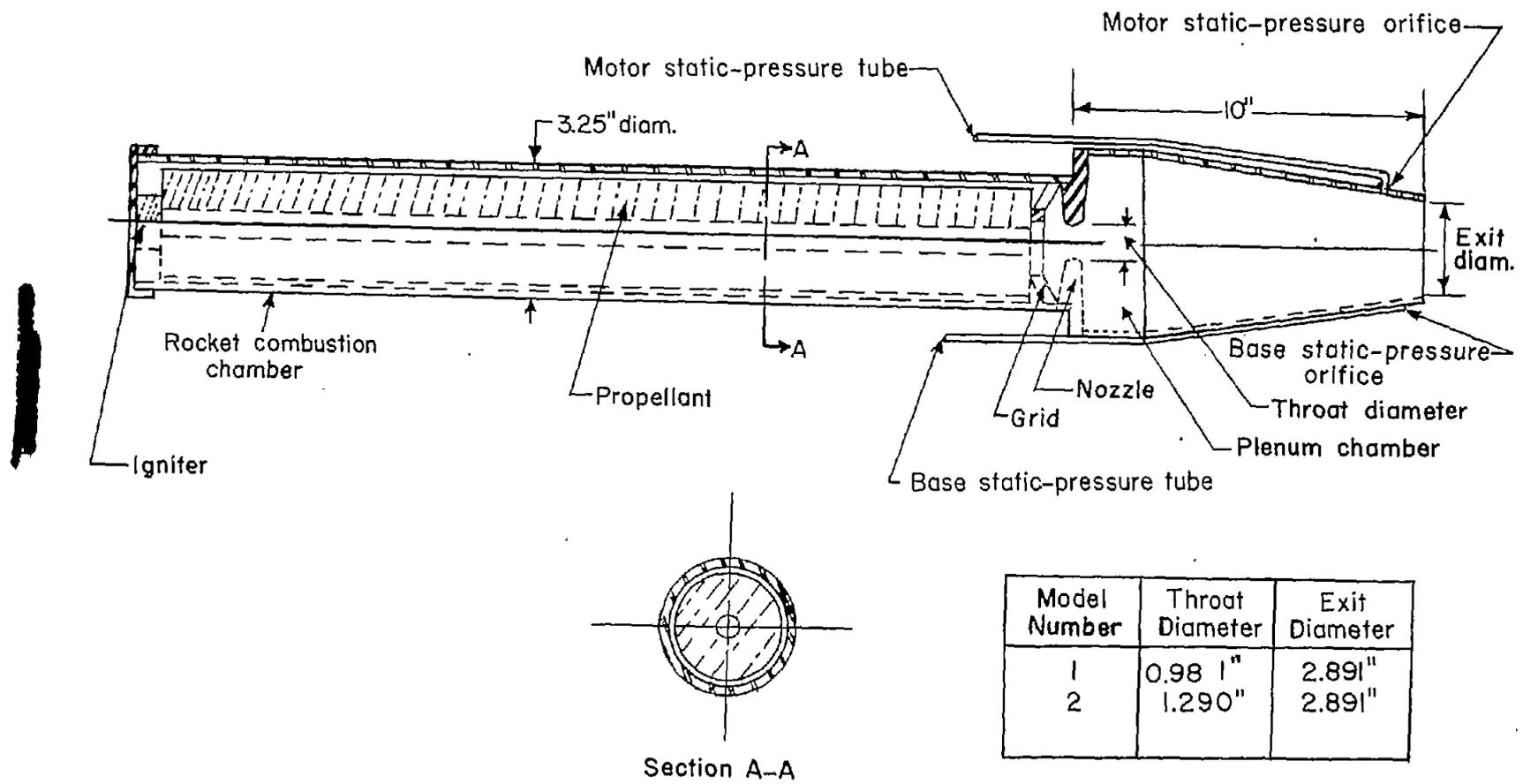
Section A-A

Figure 2.- Cross section of typical turbojet simulator.
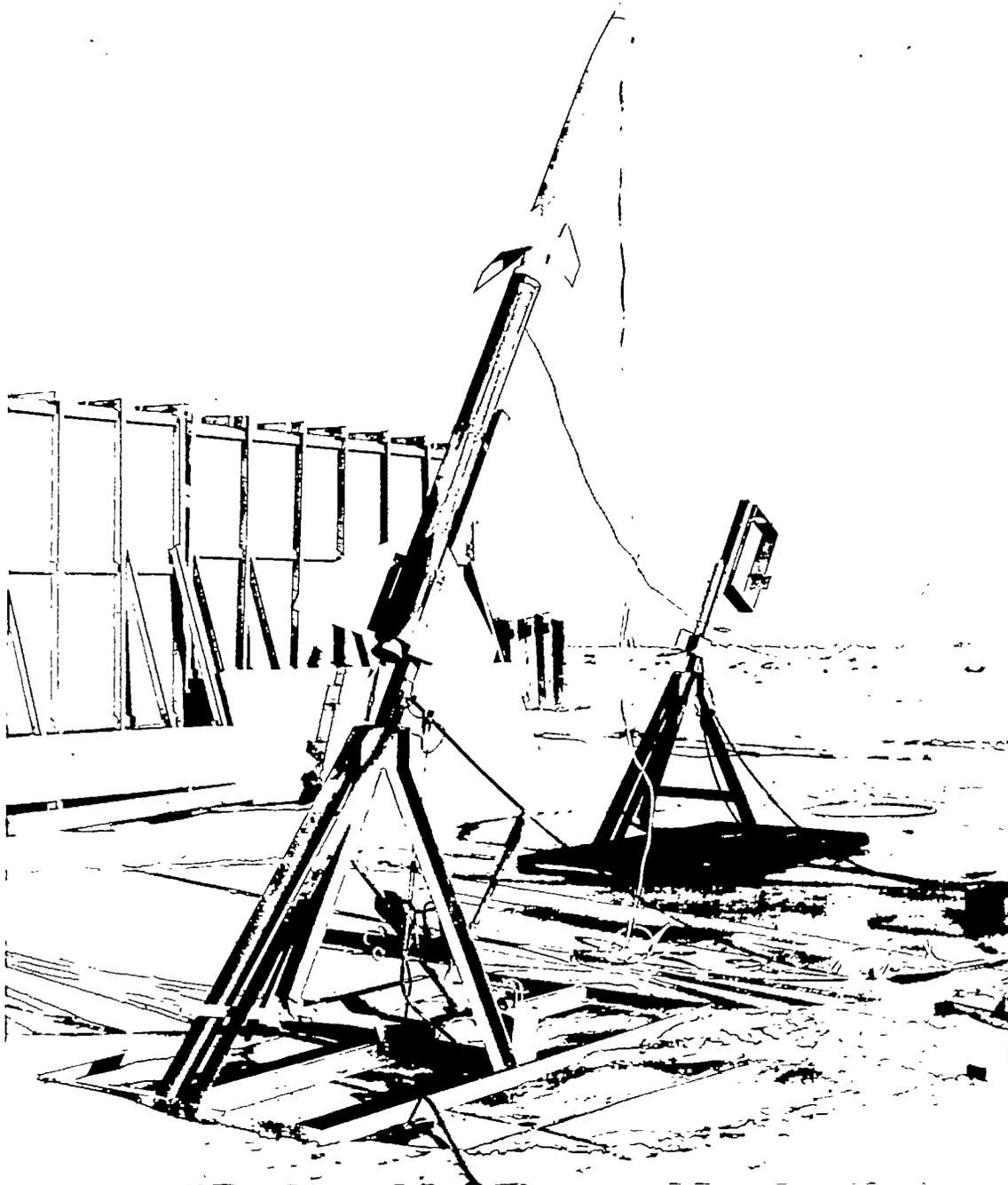
Figure 3.- Model and booster on launcher.    L-87680.1
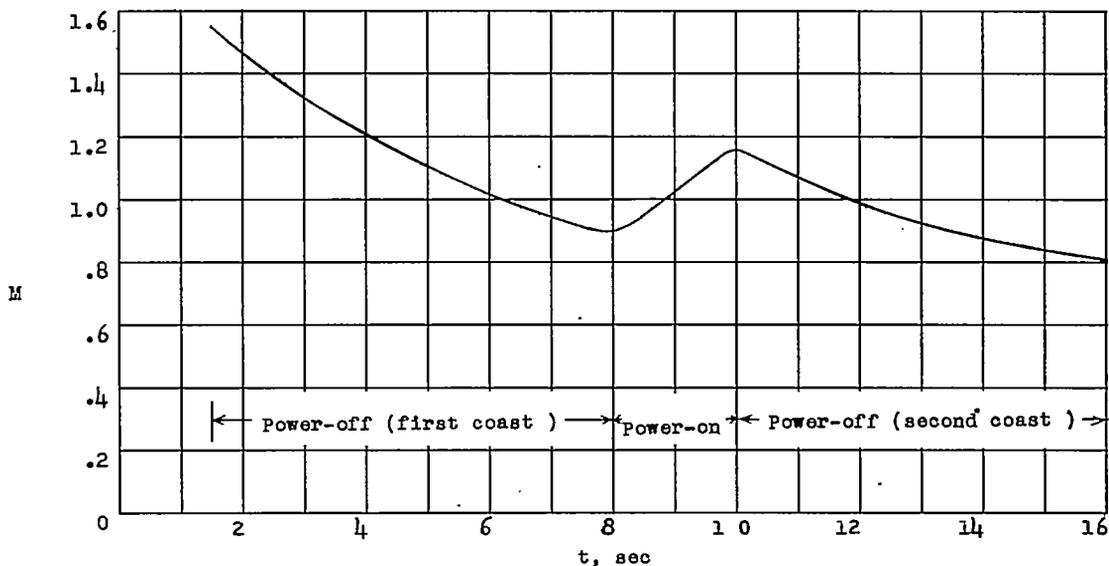
(a) Model 1.
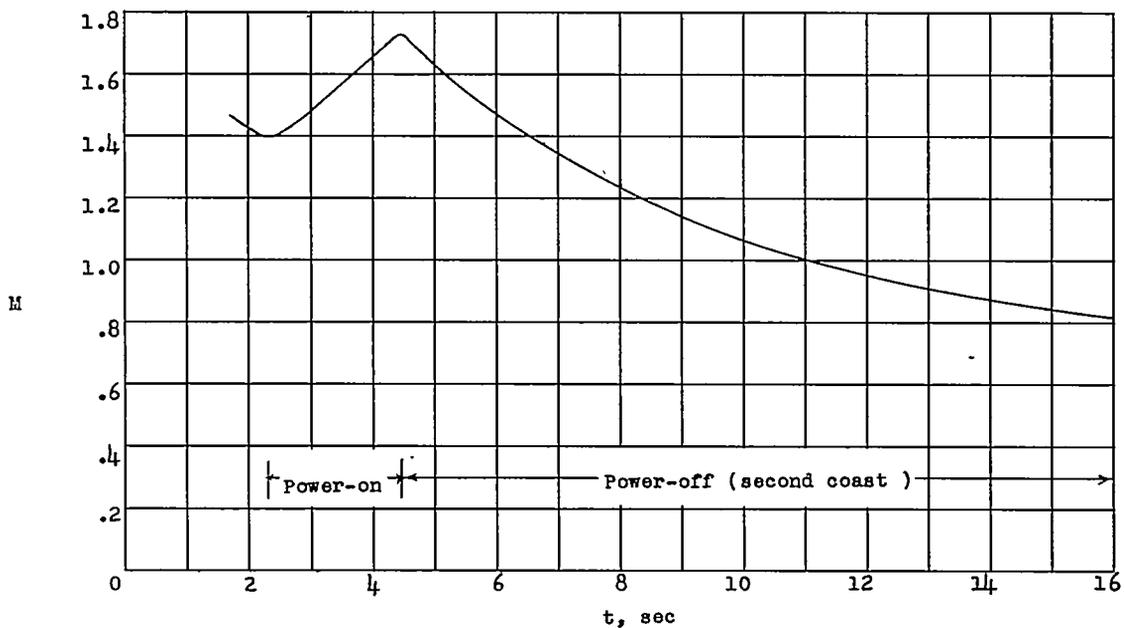


(b) Model 2.

Figure 4.- Variation of Mach number with time.
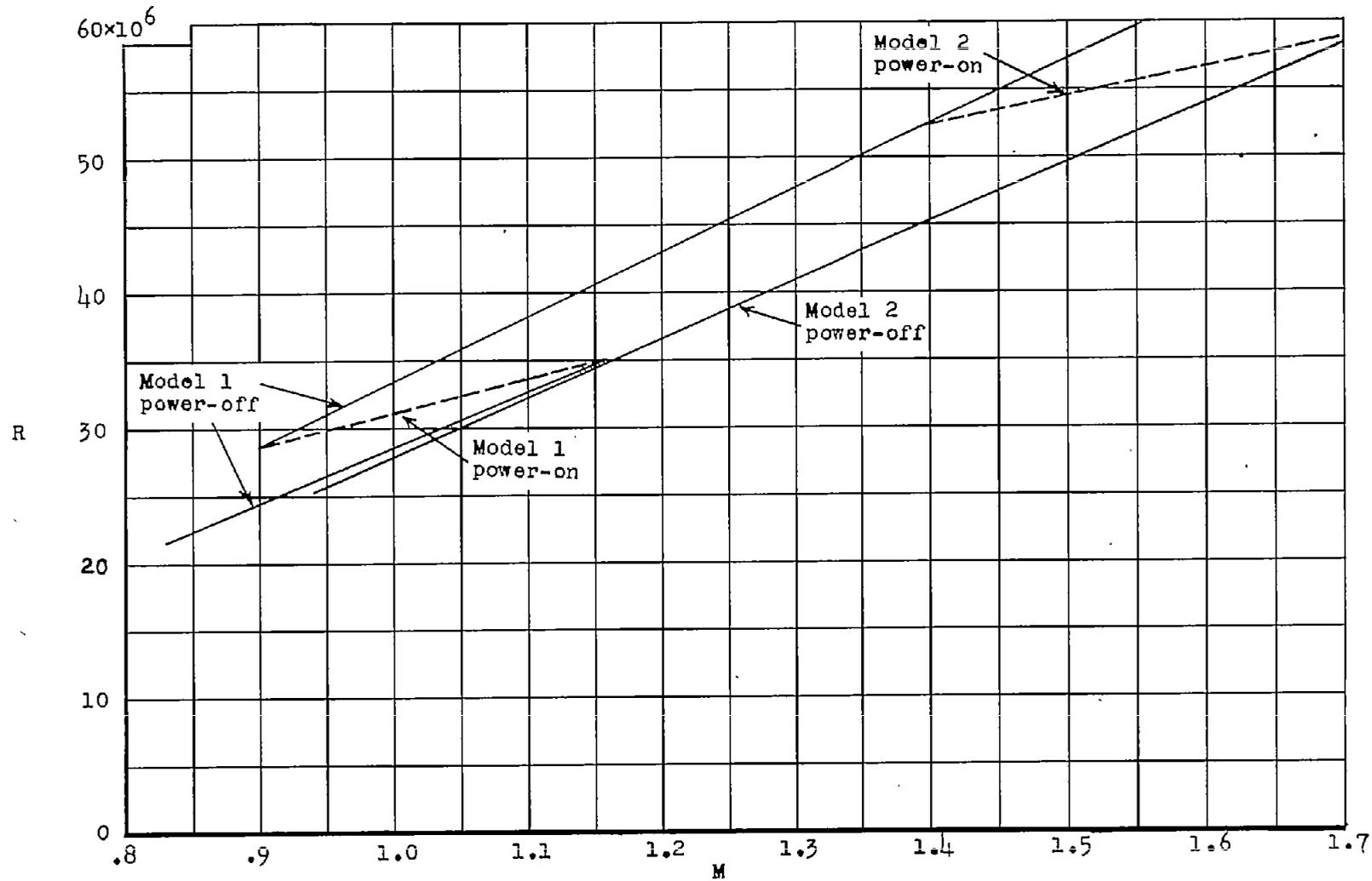
Figure 5.- Variation of Reynolds number with Mach number for models tested. Reynolds number is based on body length.

CONFIDENTIAL
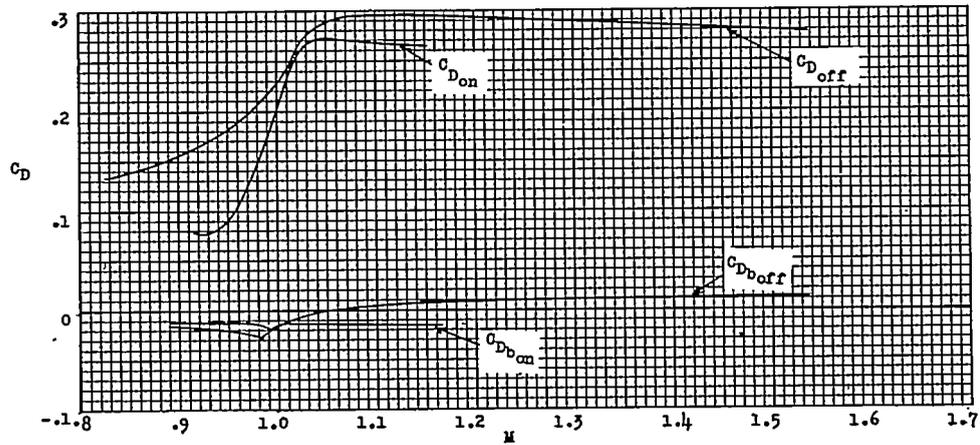


(a) Total and base drag coefficients.
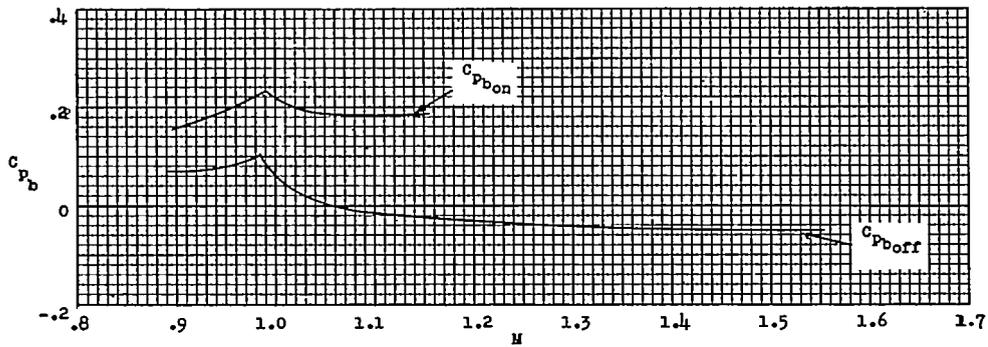


(b) Base-pressure coefficient.
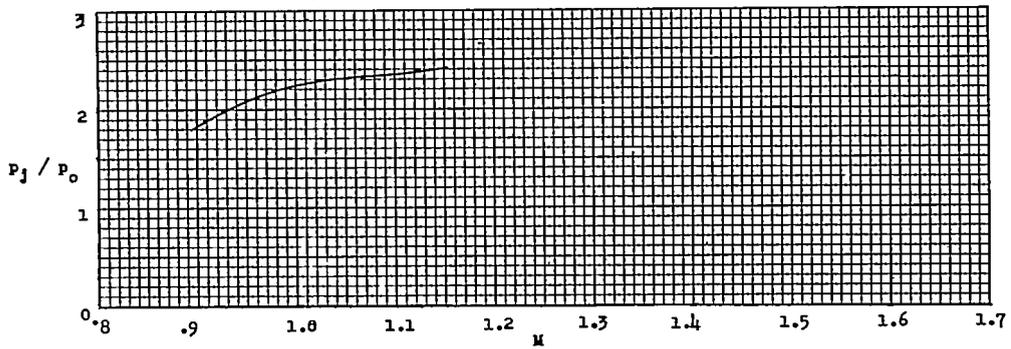


(c) Jet pressure ratio.

Figure 6.- Total and base drag coefficient, base-pressure coefficient, and jet pressure ratio as a function of free-stream Mach number. Model 1 $\left(\dfrac{A_j}{A_b} = 0.706\right)$.
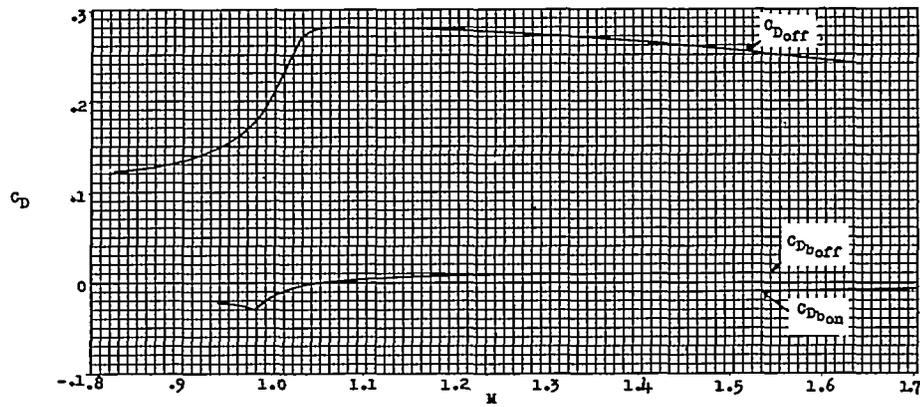
(a) Total and base drag coefficient.
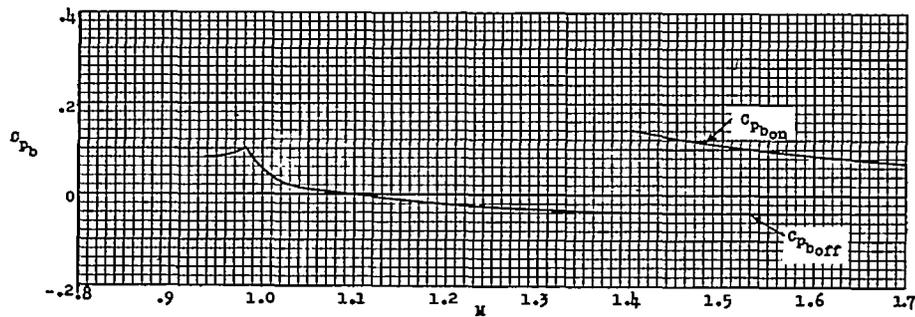


(b) Base-pressure coefficient.
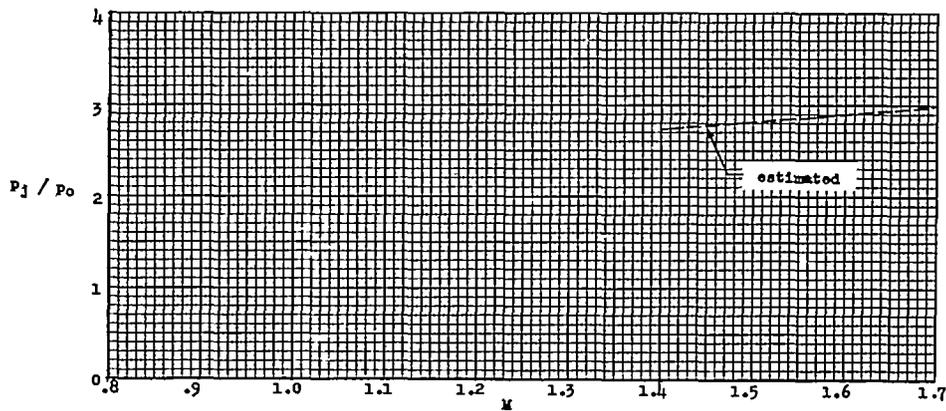


(c) Estimated jet pressure ratio.

Figure 7.- Total and base drag coefficients, base-pressure coefficient, and estimated jet pressure ratio as a function of free-stream Mach number. Model 2 $\left(\frac{A_j}{A_b} = 0.706\right)$.
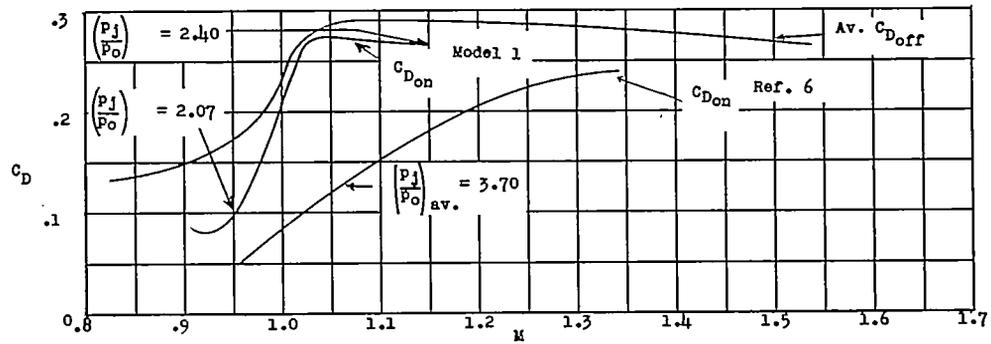
(a) Total drag coefficient.
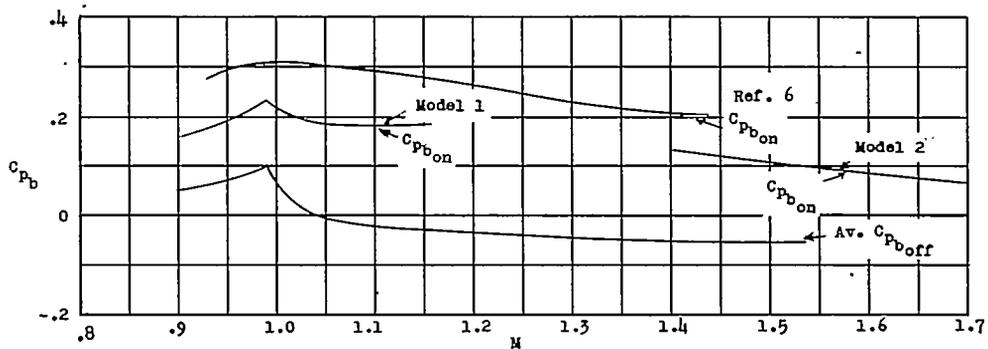


(b) Base-pressure coefficient.
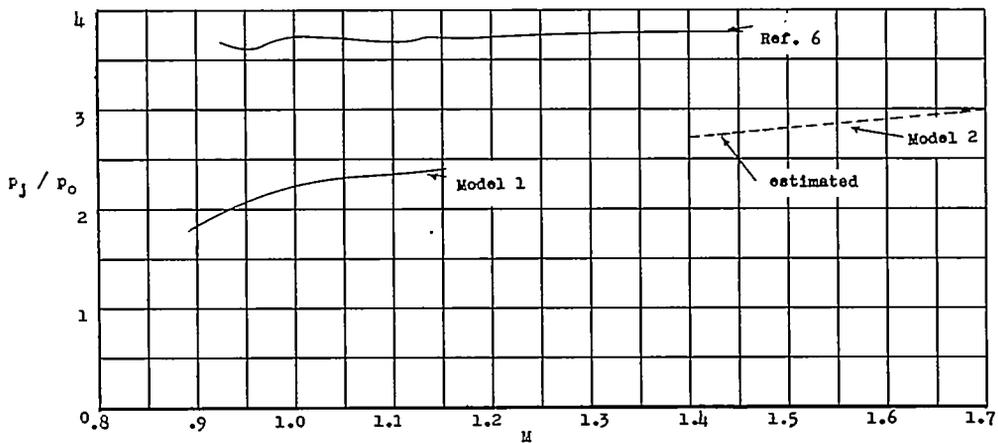


(c) Jet pressure ratio.

Figure 8.- Comparison of total drag coefficients, base-pressure coefficients and jet pressure ratios with free-stream Mach number for conical boattail bodies. $\dfrac{A_j}{A_b} = 0.706.$
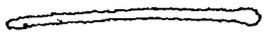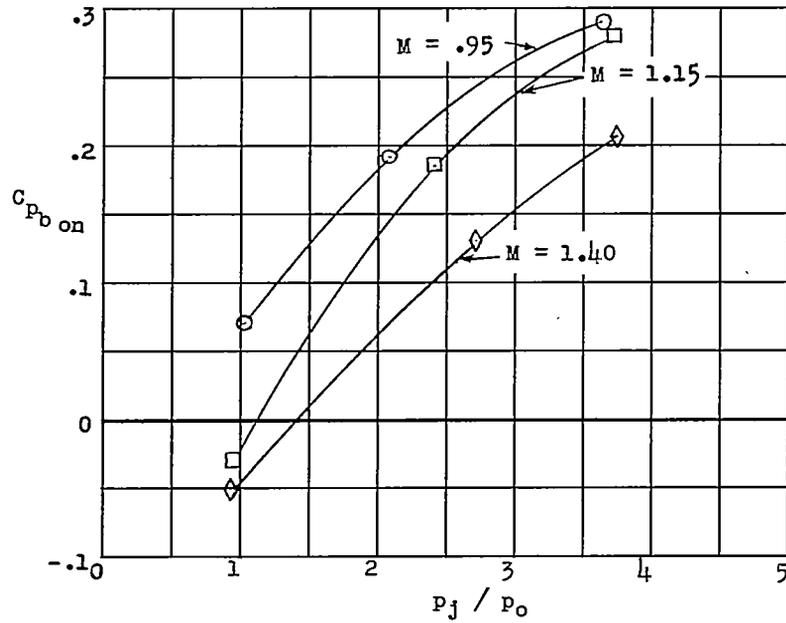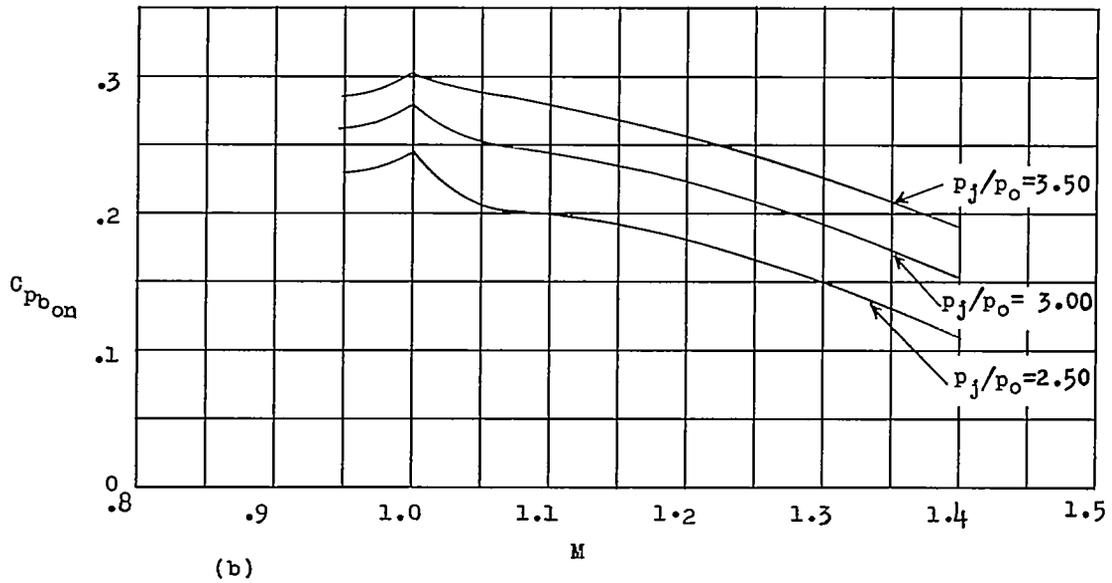
Figure 9.- Variation of power-on base pressure coefficient with jet static pressure ratio and with free-stream Mach number.